

Longitudinal, UT, and LT Variations in the Ionosphere F -Region and Plasmasphere at Minimum of Solar and Geomagnetic Activity: Similarities and Differences

Maxim V. Klimenko^{1,2}, Vladimir V. Klimenko¹, Irina E. Zakharenkova^{1,3}, Artem M. Vesnin⁴, Yury V. Yasyukevich⁵, Iuuri V. Cherniak⁶, Ivan A. Galkin⁴ and Konstantin G. Ratovsky⁵

¹West Department of Pushkov Institute of Terrestrial Magnetism, Ionosphere and Radiwave Propagation RAS, Kaliningrad, 236017, Russia

²Immanuel Kant Baltic Federal University, Kaliningrad, 236041, Russia

³Institut de Physique du Globe de Paris, 75005 Paris, France

⁴UML Center for Atmospheric Research, University of Massachusetts Lowell, 01854 Lowell, MA, USA

⁵Institute of Solar-Terrestrial Physics SB RAS, Irkutsk, 664033, Russia

⁶University of Warmia and Mazury, 10-719 Olsztyn, Poland

ABSTRACT

The most important properties of the ionosphere-plasmasphere system are its spatial and temporal variability. For interpretation and prediction of these properties global first principles, empirical and assimilation models were developed. Objective of our study is to compare the first principles Global Self-consistent Model of the Thermosphere, Ionosphere and Protonosphere (GSM TIP) and IRI Real-Time Assimilative Mapping (IRTAM) results for reproduction the main morphological features of the longitudinal, universal (UT) and local time (LT) variations in the parameters of the ionosphere-plasmasphere system. We identify the main morphology of these features of $F2$ peak critical frequency and total electron content during 2009 winter solstice.

1. INTRODUCTION

Plasma density distribution in the Earth's ionosphere-plasmasphere system plays the pivotal role in the trans-ionospheric radio waves propagation including the Global Navigation Satellite Systems performance. In order to model the ionospheric electron density we need to know the typical variations at the quiet conditions. Usually for determination of the typical (diurnal, UT or longitudinal) variations of the ionospheric parameters at different latitudes it is necessary to average these observations from the available datasets. This approach allows to separate the main temporal and spatial features of the ionosphere's variability. The obtained characteristics can be used as an input database for empirical ionospheric models like IRI [*Bilitza and Reinisch, 2008*].

Earlier it was believed that diurnal variations of the ionospheric parameters exceed significantly the longitudinal and UT variations. However, the first satellite observations disprove this [*Eccles, et al., 1971*]. In the present paper we present comparison of LT, UT and longitudinal variations to estimate their impact on the spatio-temporal distribution of the ionospheric parameters of the ionosphere-plasmasphere system.

Regardless of the recent progress on the description of the morphology of the $foF2$ and TEC longitudinal structure, there remains lack of results comparing longitudinal variations of these parameters at different latitudinal regions. One of the first results was reported in [*Clilverd, et al., 2007*] where the seasonal variations of the plasmaspheric electron density were studied at different L shells (L – McIlweine parameter). In this paper we present results of the comparison of LT, UT and longitudinal $foF2$ and TEC variations

derived for all latitudes. We analyzed data for the December 2009 solstice – the quiet geomagnetic conditions at the minimum of solar activity. We used observational results and simulated results derived from the theoretical and assimilative empirical models. This comparison allows estimation of the model performance. Often, the *TEC* variations are identified with variations of the *F2* layer critical frequency *foF2*. This statement bases on the idea of the small contribution of the plasmasphere to *TEC* and its variability. Recent investigations demonstrate that: 1) disturbances in *foF2* and *TEC* during a geomagnetic storm can be significantly different especially at a recovery phase [Cherniak, *et al.*, 2014]; 2) contribution of the topside ionosphere and plasmasphere to *TEC* results in a shift to earlier hours and weakening of the Mid-latitude Summer Evening Anomaly in *TEC* comparing to one in *foF2* [Klimenko, *et al.*, 2015]; 3) there are situations when the main contribution of *TEC* is provided by the regions above the *F2* peak [Afraimovich, *et al.*, 2011], especially during night at the solar activity minimum, where the plasmasphere's contribution to *TEC* can exceed the ionosphere's one [Cherniak, *et al.*, 2012; Klimenko, *et al.*, 2015]. Here we address the following problem. Can we use *foF2* spatial structure to construct the model of *TEC*, and vice versa can diurnal, longitudinal and UT variations of *TEC* retrieved from ground-based network of GPS receivers be applied for description of the *foF2* parameters and possible improvement of the ionosphere's empirical models, e.g. IRI?

2. METHODS

We use the set of the ionospheric data of *foF2* and *TEC* to study the diurnal, UT, latitudinal and longitudinal variations. The spatial-temporal distribution of the electron density at the heights of the ionosphere and plasmasphere can be represented as a function *f* of time and space. When we consider non-stationary processes, a function *f* in a spherical geographic coordinate system takes the form of $f(r, \theta, \lambda, t)$, where *r* is a radius vector drawn from the center of the Earth to a given point, θ is a co-latitude or a polar angle measured from the geographical North pole, $\theta = 90^\circ - \varphi$, φ is a latitude, measured from the geographical equator, λ is a geographic longitude, measured from the Greenwich meridian, *t* is a time. The *F2* layer critical frequency, *foF2*, and total electron content, *TEC*, can be considered as a function of latitude φ , longitude λ and time *t*. Time *t* can be selected as UT or LT. Averaging over UT or LT, we obtain the longitudinal variations of a considered parameter, depending on a latitude. Averaging over longitude/latitude, we obtain diurnal LT or UT variations of a considered parameter, depending on a latitude/longitude. Thus, averaging allows us to extract the main spatial and temporal features of *foF2* and *TEC*. We involved into analysis absolute total electron content data from the IGS Global Ionospheric Maps (GIM) generated on the base of world-wide network of ground-based GPS/GLONASS receivers. GIMs have spatial resolution of 5° in longitude and 2.5° in latitude and temporal resolution of 1-2 h.

3. GSM TIP MODEL BRIEF DESCRIPTION

The GSM TIP model [Namgaladze, *et al.*, 1988; Klimenko, *et al.*, 2007] was developed at the WD IZMIRAN (West Department of Pushkov Institute of Terrestrial Magnetism, Ionosphere and Radio wave propagation of the Russian Academy of Sciences). It was used for simulations of the time-dependent global structure of the near-Earth space environment from 80 km to 15 Earth radii. In the thermospheric block of the model, global distribution of the neutral gas temperature (T_n) and of N_2 , O_2 , O , NO , $N(^4S)$, and $N(^2D)$ densities, as well as the three-dimensional circulation of the neutral gas and N_2^+ , O_2^+ , and NO^+ , and also their temperature (T_i) and velocities (V_i), are calculated in the range from 80 to 526 km in a spherical geomagnetic coordinate system. In the ionospheric section of the model the global time-dependent distributions of ion and electron temperatures (T_i , T_e), vector velocity (V_i), and O^+ and H^+ ion concentrations are calculated in a magnetic dipole coordinate system from 175 km in the Northern hemisphere to 175 km in the Southern hemisphere. In this case, the ionosphere code for atomic ions does not require an upper boundary condition. The total electron content (*TEC*) in the GSM TIP model is calculated by integration of the electron density from bottomside ionosphere to the altitude of GPS/GLONASS satellites (20,200 km). Additionally, the model also provides the potential distribution of the two-dimensional electric field of ionospheric and magnetospheric origin. The Earth's magnetic field is approximated by a tilted dipole.

The GSM TIP model takes into account the mismatch between geographic and geomagnetic axes, as well as dynamical processes in ionosphere-plasmasphere system such as (1) plasma transport along geomagnetic field lines produced by thermospheric winds through neutral-ion collisions, (2) the zonal and meridional

electromagnetic plasma drift. It should be noted that this feature and processes must always be taken into account in first principles models for adequate description of the longitudinal and UT variations in ionospheric and plasmaspheric electron density. GSM TIP model has already been used to study the longitudinal and UT variations of equatorial electrojet [Klimenko, *et al.*, 2007], mid latitude and sub-auroral anomalies in F_2 region electron density in separated longitudes [Klimenko, *et al.*, 2015]. We tried to identify the main morphological features of the longitudinal, UT and LT variations in F peak critical frequency and total electron content during 2009 winter solstice during solar activity minimum. For this reason the GSM TIP run was carried out for quiet solstice conditions on December 22, 2009 without taking into account mesospheric tides on the lower boundary of the model (80 km).

4. IRTAM MODEL BRIEF DESCRIPTION

The second model that we used is IRI-based Real-Time Assimilative Mapping (IRTAM) [Galkin, *et al.*, 2012]. IRTAM uses measurements from the Global Ionosphere Radio Observatory (GIRO) and knowledge about ionospheric climatology to now-cast global ionospheric weather. The IRTAM morphs the empirical “climatology” IRI model into agreement with the GIRO measurements, so that the new model representations of the ionosphere closely follow its “weather” variability. For IRTAM, relative simplicity of the underlying model formalism in comparison to the physics-based models has allowed computations to span past history of model-vs-observation behavior for up to 24 hours. By using 24 hour history of observations rather than one latest measurement we ensure IRTAM robustness to data gaps and autoscaling errors.

IRTAM uses same formalism to represent every ionospheric parameter (foF_2 , h_mF_2 and etc.) and calculate separate representation (coefficient set) for each of them. Magnetic field is accounted in IRTAM (as well as in IRI) by the use of International Reference Magnetic Field (IGRF) model. Thus, IRTAM accounts for precise position of the magnetic equator that is very important to accurately reproduce ionospheric features at low latitudes. 12-month running mean sunspot number, $R_{z,12}$, does not have role of the driver for IRTAM modeling (that important role it played in IRI), since all effects due to solar activity are “built-in” observational data. In the regions where there is no GIRO ionosondes IRTAM modeling results are close to IRI results. Thus for correct IRTAM maps interpretation one should know which data came into the assimilation. This is not major issue, since IRTAM coefficients come together with assimilated data. IRTAM only uses IRI climatology representation, IGRF magnetic field representation and observational data to do the computations. Since each of these three components is reliable IRTAM maps are also reliable, given a good data coverage.

5. RESULTS AND DISCUSSION

In this section we present comparison of GSM TIP and IRTAM computations for foF_2 as well as comparison of GSM TIP computation and GPS observations for TEC . All data correspond to December 22, 2009. We performed different averaging, as discussed above, to study spatial and temporal morphological features. As assimilative model, IRTAM relies on the measurements of GIRO ionosonde network. The spatial coverage of data for December of 2009 is better for northern hemisphere, than for southern. Thus the quality of IRTAM maps is better in northern hemisphere and IRTAM maps for southern hemisphere should be analyzed with cautious.

Figure 1 top panels show foF_2 dependence on local time and geographical latitude averaged over longitude, which we refer as LT variations. These maps are produced as follows: 1) we calculated 24 (1 hour resolution) foF_2 global maps with spatial resolution 15° by longitude and 5° by latitude for particular local time, hence we have 24 global maps; 3) we took average value at each latitude, joint all latitudinal profiles according to local time variation and the result is shown in Figure 1. Similar set of manipulation were takes to produce TEC maps. GSM TIP and IRTAM foF_2 maps qualitative agree with each other as well as GPS TIP and GPS TEC maps. Moreover foF_2 and TEC maps show mostly the same features except for the equatorial ionosphere and high-latitude regions. Since LT variations of foF_2 and TEC mostly correlate, this means that LT variations of TEC in quiet geomagnetic conditions are mainly controlled by F region ionospheric plasma. The discrepancy between TEC and foF_2 can be basically explained by smoothing ionospheric features (foF_2) by plasmasphere in TEC . Thus, equatorial anomaly crests and main ionospheric thorough are seen mainly in foF_2 maps and are smoothed out in TEC maps. It is worth noting that in Figure 1 and in the other figures

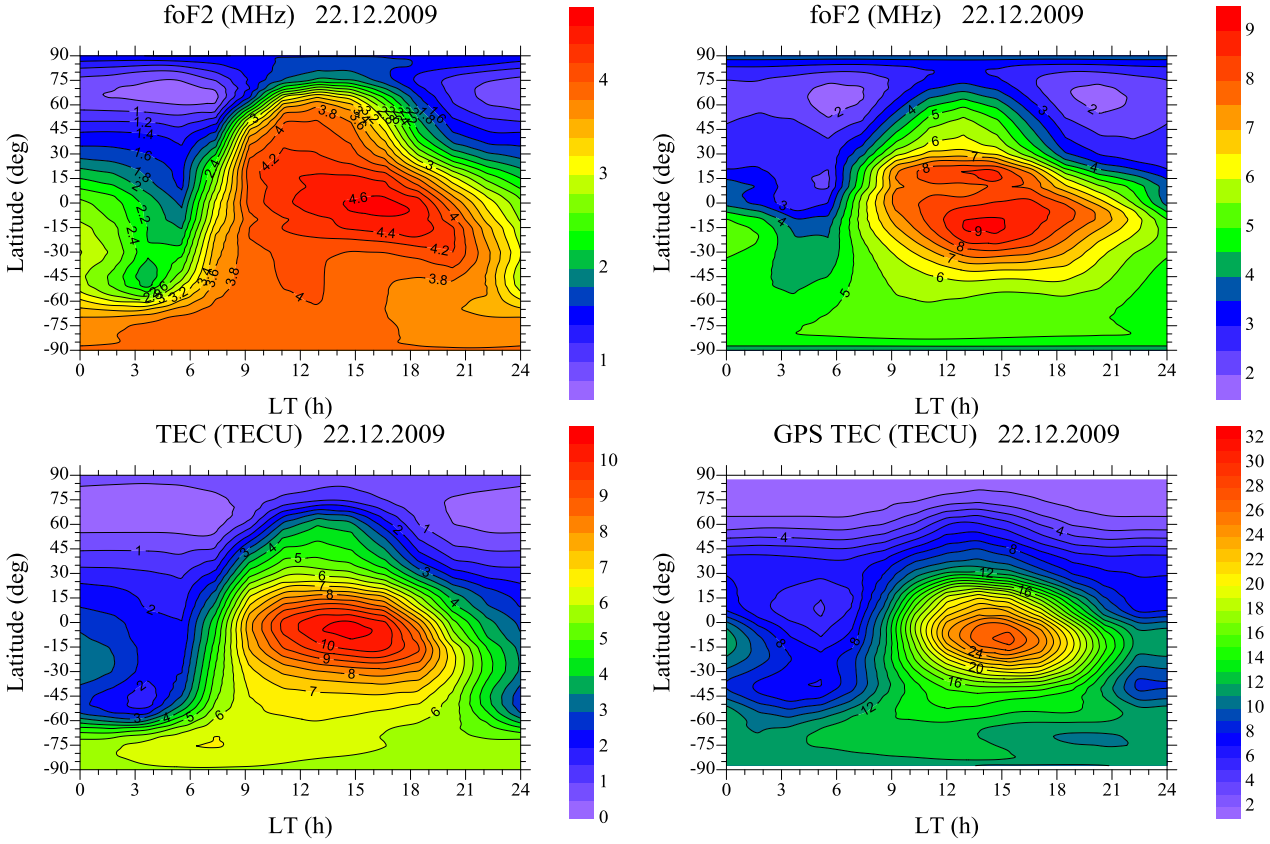


Figure 1. LT variations of f_oF_2 and TEC on different latitudes. Maps show f_oF_2 and TEC on latitude – local time grid with 5° latitude step and 1 hour time step. Data are averaged by longitude for day December 22 2009. Top panels show f_oF_2 variations based on the computations of GSM TIP (left) and IRTAM (right). Bottom panels show TEC variations based on computations of GSM TIP (left) and GPS measurements (right).

f_oF_2 values calculated using GSM TIP and IRTAM are only qualitatively agree with each other. Quantitatively GSM TIP routinely shows underestimated f_oF_2 and TEC. The reason for that is overestimate neutral atmosphere concentration in GSM TIP, which causes higher recombination rate and lower plasma density. We suggested that it does not qualitatively affect the f_oF_2 and TEC distributions.

Figure 2 recapitulates longitude variations of f_oF_2 and TEC. This is similar to LT variation except for now we averaged data over time (LT or UT does not matter since we consider 24 hours time interval) at the same longitude. In high-latitude region down to $\sim 55^\circ\text{N}$ major features are polar ionospheric cavity and main ionospheric trough. Both GSM TIP and IRTAM depict each of them. Polar ionospheric cavity appears at 290°E and 270°E longitude in GSM TIP and IRTAM maps correspondingly, also it is more pronounced in GSM TIP map rather than IRTAM map. Main ionospheric trough appears to have minimum at 75°N , 130°E as modeled by GSM TIP and at 75°N , 110°E as mapped by IRTAM. In mid-latitude and low-latitude regions GSM TIP draws one maximum in f_oF_2 distribution, but IRTAM draws several such maximums. This discrepancy can be caused by the limitations of either of the models. On the one hand GSM TIP accounts for the magnetic field as for the simple dipole-like field and also does not take into account thermospheric tides. On the other hand IRTAM depends on data coverage. Data sources in northern hemisphere are mainly concentrated in three sectors: North American, European and Asian. Hence, observed maximum might be the artifacts of non-uniform data coverage. Both models reproduce minimum of f_oF_2 in ionospheric anomaly well, except the topology magnetic field is more accurately reproduce in IRTAM. Also, GSM TIP and IRTAM show the greatest development of equatorial anomaly crests appearance nearly in the same longitudinal region: (240°E – 300°E) for GSM TIP and (210°E – 270°E) for IRTAM. GSM TIP and IRTAM

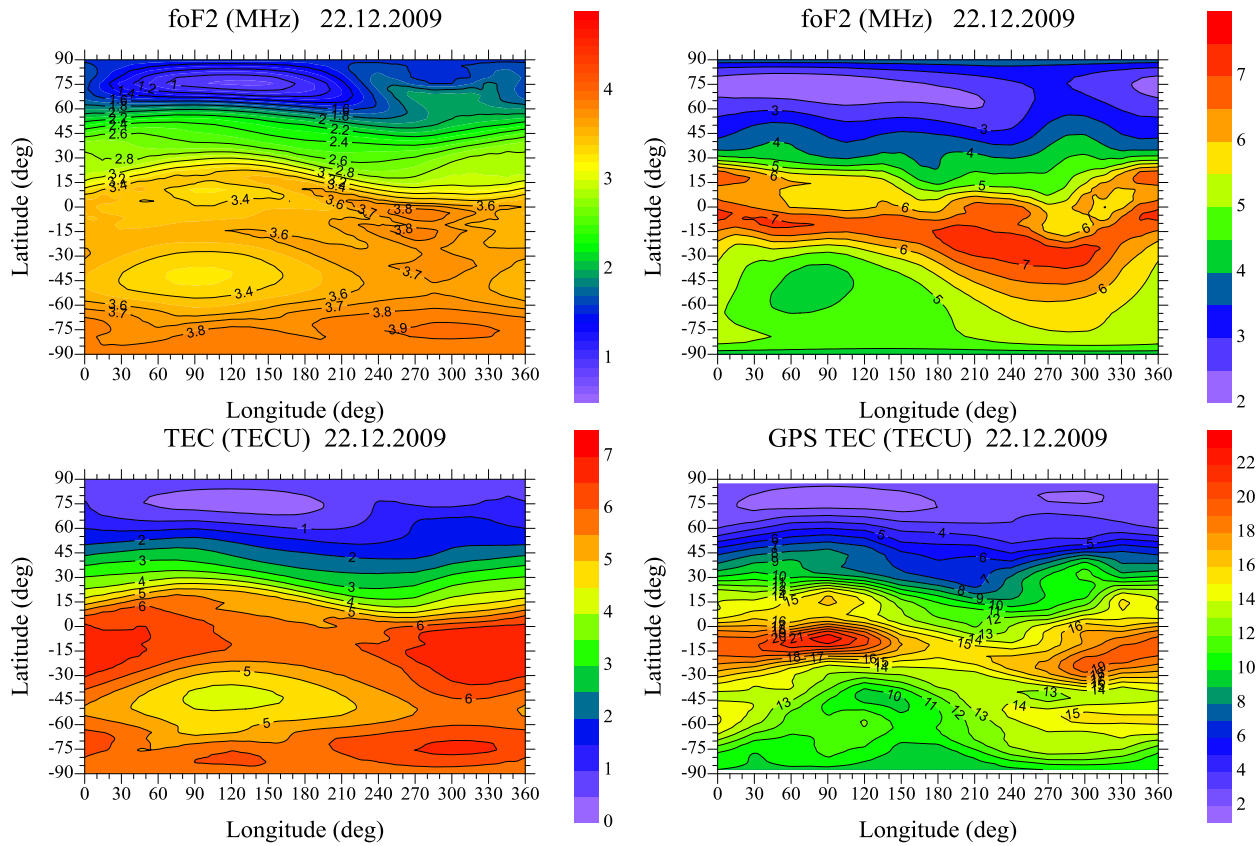


Figure 2. Longitude variations of $foF2$ and TEC on different latitudes. Maps show $foF2$ and TEC on latitude – longitude grid with 5° latitude step and 15° longitude step. Data are averaged by time for December 22, 2009. Top panels show $foF2$ variations based on the computations of GSM TIP (left) and IRTAM (right). Bottom panels show TEC variations based on computations of GSM TIP (left) and GPS measurements (right).

also show good agreement in southern hemisphere. Minimum of $foF2$ distribution is located at $(45^\circ\text{S}, 90^\circ\text{E})$ and maximum is located in longitudinal range $220^\circ\text{E}–330^\circ\text{E}$. The difference in GPS TIP and IRTAM simulations appears in high-latitude region of southern hemisphere. GSM TIP draws the maximum at $(75^\circ\text{S}, 300^\circ\text{E})$ and IRTAM does not show same feature. We explain it by the insufficient data coverage in this region. Maximum of $foF2$ in southern hemisphere is located in American longitudinal sector. Moreover, longitudinal total content of F region ionospheric plasma is greater for American sector at any LT which is shown by Figure 3. It should be noted the difference between $foF2$ and TEC distributions, shown in Figure 3, which consists in a different longitudinal position of the daytime $foF2$ and TEC maxima. Thus, the $foF2$ maximum is formed in the American longitudinal sector ($\sim 300^\circ$), and TEC maximum is formed in the Atlantic sector ($\sim 340^\circ$). The latitudinal structure of this ionospheric plasma maximum is more complex as simulated by GSM TIP, rather than IRTAM (Figure 2). GSM TIP reveals several maximum in different latitudinal region caused by different mechanisms.

Longitude variations of TEC as modeled by GSM TIP and as shown by observations agree with each other, which do not hold for $foF2$ and TEC longitude variations. One model/data discrepancy is that high-latitude summer maximum of TEC in observations is at $\sim 60^\circ\text{S}$ and GSM TIP shows it at 75°S . Another issue is about relative distribution of $foF2$ and TEC in high-latitude region of southern hemisphere and equatorial ionosphere. Although, plasma density in southern hemisphere is greater than the density in northern hemisphere, which is reasonable since southern hemisphere is subjected to more solar ionizing radiation (December corresponds to summer in southern hemisphere), we can see that $foF2$ and TEC are even higher at high latitudes of southern hemisphere than in low-latitude equatorial ionosphere. This result should be subjected to further study and is not discussed in the details in this paper. In this study we only perform qualitative comparison. High-latitude TEC maximum in American longitude sector which is seen by GPS

observations and reproduced by GSM TIP can indirectly point out that $foF2$ result should also show a maximum in spatially close to TEC maximum. Such a maximum appears to be on the right place on GSM TIP maps, but is absent on IRTAM maps, which is again can be attributed to insufficient data coverage.

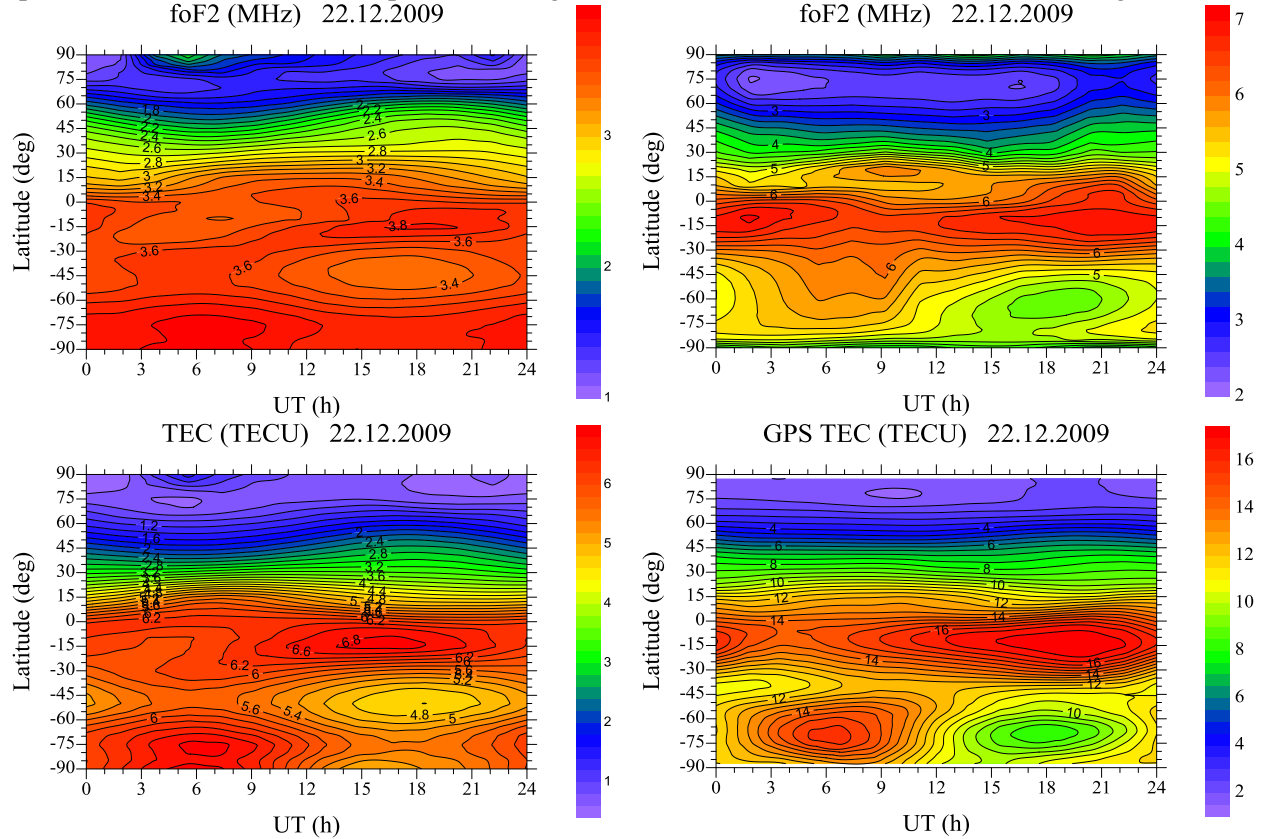


Figure 3. UT variations of $foF2$ and TEC on different latitudes. Maps show $foF2$ and TEC on latitude – universal time grid with 5° latitude step and 1 hour time step. Data are averaged by longitude for day December 22, 2009. Basically data at each UT hour are results of compression of entire global map to a single slice (column). Top panels show $foF2$ variations based on the computations of GSM TIP (left) and IRTAM (right). Bottom panels show TEC variations based on computations of GSM TIP (left) and GPS measurements (right).

Figure 4 shows the UT variations of the $foF2$ and TEC latitudinal structure, time-averaged per day on December 22, 2009. The value of the $foF2$ and TEC UT variations in the northern (winter) hemisphere is very small. In the GSM TIP model the $foF2$ and TEC UT-variations in the southern (summer) hemisphere reveal the similar morphological features: 1) the near-equatorial maximum at 16:00–19:00 UT and minimum at 06:00–07:00 UT; 2) the mid-latitude transition region with a minimum forming in the latitudinal distribution, with a maximum at 06:00 UT and a minimum at 18:00 UT; 3) the high-latitude maximum at 06:00 UT and minimum at 18:00 UT. The same features are also manifested in the IRTAM model calculation results and GPS TEC observation data with the only difference being that: 1) in the high latitudes of the Southern (summer) hemisphere according to the IRTAM model the $foF2$ longitudinal maximum is formed, however, the maximum is not formed in the $foF2$ latitudinal distribution; 2) in the GPS TEC data we can not clearly distinguish the mid-latitude structure of the UT variations.

Comparing Figures 1, 2 and 4, we can see that longitude, UT and LT variations of $foF2$ and TEC are of the same order except for equatorial region. In equatorial ionosphere $foF2$ and TEC are the largest around local noon and exceed values at different locations by the order of magnitude. Morphological features of $foF2$ and

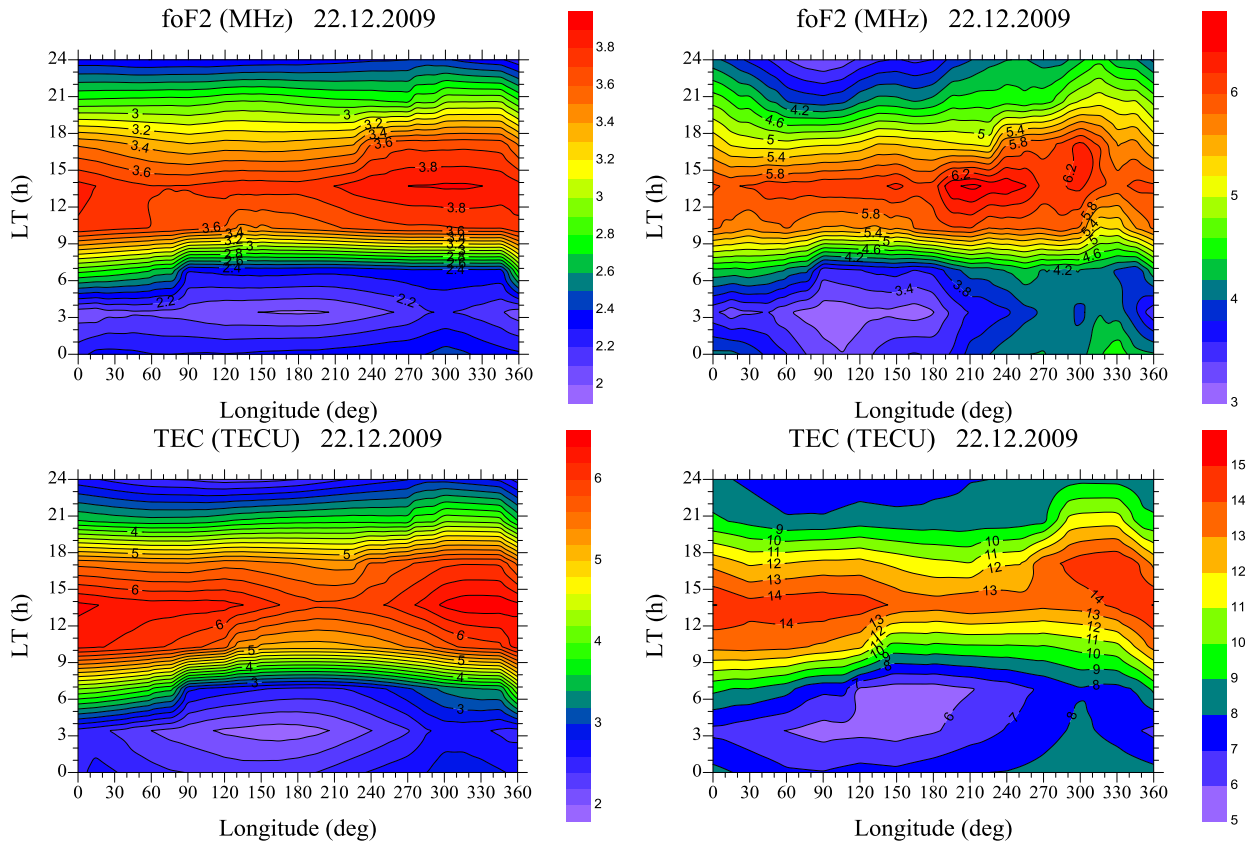


Figure 4. Longitude variations of $foF2$ and TEC on different local times. Maps show $foF2$ and TEC on local time – longitude grid with 1 hour time step and 15° longitude step. Data are averaged by latitude for day December 22 2009. Top panels show $foF2$ variations based on the computations of GSM TIP (left) and IRTAM (right). Bottom panels show TEC variations based on computations of GSM TIP (left) and GPS measurements (right).

TEC are in agreement with each other. Thus, we can conclude that the ionosphere is a main source of TEC variations under geomagnetic quiet condition. This is reasonable since the plasmasphere, another contributor to TEC , should not vary much during geomagnetic quiet time.

6. SUMMARY

Here we analyze the main morphological features of latitudinal, longitudinal, UT and LT $foF2/TEC$ variations for the conditions of December of 2009 solstice. Comparison of these variations in TEC and $foF2$ demonstrates that in general, they are identical and interchangeable in the context of the construction an empirical model of these parameters for quiet geomagnetic conditions. Longitudinal, UT and LT variations in both $foF2$ and TEC are comparable in the order of magnitude everywhere, except the region of the equatorial ionization anomaly, where LT variation is one order of magnitude larger than UT and longitudinal variations. Besides, at the middle and high latitudes of the Southern (summer) hemisphere the values of the longitudinal, UT and LT variations are most similar to each other. According to the model calculations derived from GSM TIP and IRTAM, as well as GIM data the maxima in $foF2$ and TEC are formed at all latitudes in the American longitudinal sector of the Southern (summer) hemisphere. In the American longitudinal sector we can distinguish the near-equatorial and high-latitude maxima in the latitudinal structure of $foF2$ and TEC . The plasma density in the ionosphere is generally greatest in the American longitudinal sector at any LT. Formation of the high-latitude maximum in GPS TEC over the American longitudinal sector presents an indirect confirmation of the fact that high-latitude maximum in $foF2$ should be also present in an empirical model of the ionosphere.

ACKNOWLEDGEMENTS

We are grateful to International GNSS Service (IGS) for GPS data and products (<ftp://cddis.gsfc.nasa.gov/pub/gps/>). This study was financially supported by Grants from the President of the Russian Federation MK-4866.2014.5 (M.V. Klimenko, I.E. Zakharenkova) and RFBR No. 14-05-00788 (V.V. Klimenko, K.G. Ratovsky, Yu.V. Yasyukevich).

REFERENCES

- Afraimovich, E.L., Astafyeva, E.I., Kosogorov, E.A., & Yasyukevich, Yu.V. (2011). The mid-latitude field-aligned disturbances and its impact on differential GPS and VLBI. *Advances in Space Research*, 47, 1804–1813, doi:10.1016/j.asr.2010.06.030.
- Bilitza, D., & Reinisch, B.W. (2008). International Reference Ionosphere 2007: Improvements and new parameters. *Advances in Space Research*, 42(4), 599–609, doi: 10.1016/j.asr.2007.07.048
- Cherniak, Iu.V., Zakharenkova, I.E., Krankowski, A., & Shagimuratov, I.I. (2012). Plasmaspheric electron content derived from GPS TEC and FORMOSAT-3/COSMIC measurements: solar minimum conditions, *Advances in Space Research*, 50(4), 427–440, doi: 10.1016/j.asr.2012.04.002.
- Cherniak, Iu.V., Zakharenkova, I.E., Dzubanov, D., & Krankowski, A. (2014). Analysis of the ionosphere/plasmasphere electron content variability during strong geomagnetic storm. *Advances in Space Research*, 54(4), 586–594, doi: 10.1016/j.asr.2014.04.011.
- Clilverd, M.A., Meredith, N.P., Horne, R.B., Glauert, S.A., Anderson, R.R., Thomson, N.R., Menk, F.W., & Sandel, B.R. (2007). Longitudinal and seasonal variations in plasmaspheric electron density: Implications for electron precipitation. *Journal of Geophysical Research*, 112, A11210, doi:10.1029/2007JA012416.
- Eccles, D., King, J.W., & Rothwell, P. (1971). Longitudinal variations of the mid-latitude ionosphere produced by neutral-air winds – II. Comparisons of the calculated variations of electron concentration with data obtained from the Ariel I and Ariel III satellites. *Journal of Atmospheric and Terrestrial Physics*, 33(3), 371–377.
- Galkin, I.A., Reinisch, B.W., Huang, X., & Bilitza, D. (2012). Assimilation of GIRO data into a real-time IRI. *Radio Science*, 47, RS0L07, doi:10.1029/2011RS004952.
- Klimenko, M.V., Klimenko, V.V., & Bryukhanov, V.V. (2007). Numerical modeling of the equatorial electrojet UT-variation on the basis of the model GSM TIP. *Advances in Radio Science*, 5, 385–392.
- Klimenko, M.V., Klimenko, V.V., Karpachev, A.T., Ratovsky, K.G., & Stepanov, A.E. (2015). Spatial features of Weddell Sea and Yakutsk Anomalies in f_oF2 diurnal variations during high solar activity periods: Interkosmos-19 satellite and ground-based ionosonde observations, IRI reproduction and GSM TIP model simulation. *Advances in Space Research*, 55(8), 2020–2032, doi:10.1016/j.asr.2014.12.032.
- Klimenko, M.V., Klimenko, V.V., Ratovsky, K.G., Zakharenkova, I.E., Yasyukevich, Yu.V., Korenkova, N.A., Cherniak, I.V., & Mylnikova, A.A. (2015). Mid-latitude Summer Evening Anomaly (MSEA) in $F2$ layer electron density and total electron content at solar minimum. *Advances in Space Research* (in print).
- Klimenko, M.V., Klimenko, V.V., Zakharenkova, I.E., & Cherniak, Iu.V. (2015). The global morphology of the plasmaspheric electron content during Northern winter 2009 based on GPS/COSMIC observation and GSM TIP model results. *Advances in Space Research*, 55(8), 2077–2085, doi:10.1016/j.asr.2014.06.027.
- Namgaladze, A.A., Korenkov, Yu.N., Klimenko, V.V., Karpov, I.V., Bessarab, F.S., Surotkin, V.A., Glushchenko, T.A., & Naumova, N.M. (1988). Global model of the thermosphere-ionosphere-protonosphere system. *Pure and Applied Geophysics*, 127(2/3), 219–254.